ISSN: 0067-2904

Impact of Porous Media on Peristaltic Transport of Tangent Hyperbolic Nanofluid in Asymmetric Channel

Aqeel J. Hashim,* Ahmed M. Abdulhadi
Department of Mathematics, College of Science, University of Baghdad, Baghdad, Iraq

Received: 15/2/2023 Accepted: 22/4/2023 Published: 30/1/2024

Abstract

The purpose behind this paper is to discuss nanoparticles effect, porous media, radiation and heat source/sink parameter on hyperbolic tangent nanofluid of peristaltic flow in a channel type that is asymmetric. Under a long wavelength and the approaches of low Reynolds number, the governing nanofluid equations are first formulated and then simplified. Associated nonlinear differential equations will be obtained after making these approximations. Then the concentration of nanoparticle exact solution, temperature distribution, stream function, and pressure gradient will be calculated. Eventually, the obtained results will be illustrated graphically via MATHEMATICA software.

Keywords: Peristaltic transport, nanofluid, thermal conductivity, porous media, tangent hyperbolic nanofluid, a symmetric channel, wavelength number

تأثير الوسط المسامي في جريان تمعجي لمائع من النمط THN في قناة غير متناظرة

عقيل جبار هاشم *, احمد مولود عبد الهادي
قسم الرياضيات , كلية العلوم , جامعة بغداد , بغداد , العراق

الخلاصة :

الهدف من هذا البحث هو مناقشة تأثير الجسيمات النانوية , الوسائط المسامية , معلمة الحرارة , وألاشعاع على التدفق التمعجي لسائل من نوع THN في قناة غير متناظرة. تحت تاثير طول موجي طويل وعدد تقريبي صغير لرايونلدز , تتم أولا صياغة المعادلات ألاساسية للموائع النانوية ثم يتم تبسيطها. وبعد اجراء هذه التقديرات التقريبية سيتم الحصول على المعادلات التفاضلية غير الخطية. بعد ذلك سيتم حساب الحلول الدقيقة لتركيز الجيسمات النانوية وتوزيع درجة الحرارة ودالة التدفق وتدرج الضغط. في النهاية , سيتم توضيح النتائج التي تم الحصول عليها بيانيا بواسطة برنامج ماثماتيكا.

1. Introduction

In this research the phenomenon of peristaltic is going to be explained as a phenomenon in which the transport of material induced along the length of distensible tube via a continuous wave of shrinking and extension, in the direction of the wave propagation, mingling and conveying the fluid. Swallowing of food through esophagus, the movement of chyme in the gastrointestinal tracts, urine transport from kidney to bladder, and the vasomotion of small blood vessels are all examples of the role of peristaltic in transporting physiological fluids in

*Email: oqil.jabbar1203a@sc.uobaghdad.edu.iq

the body. Several recent equipment has been invented depending on the idea of peristaltic pumping for transporting fluids without inner moving parts. For instance, blood pumping in heart-lung machine.

Peristaltic transport has been investigated by many authors such as Abdulhadi and Sabah [1], Abdulhadi and Morad [2], Abdulhadi and Fat'hy [3], Abdulhadi and Qabas [4], Many other investigators have been attracted by the mechanism of peristaltic transport in different situations. With referring to physiological and mechanical conditions, the peristaltic flow for different fluids has been reported. In majority of these studies, the peristaltic flow in a symmetric kind of channel is confined. In this research, nanofluid is also going to be clarified as a fluid containing small amount of uniformly dispersed and suspended nanometer-sized particles in base fluid. The fluid thermal conductivity is improved when a small number of nanoparticles is appended to the basis fluid, in this case the fluid is named nanofluid which was first coined by Choi (1995). In addition to, porous media has been introduced as 'the ratio of the pores volume compared to total bulk media volume '. (often explained as fragment or percent).

The aim of this paper is to investigate the peristaltic transport of tangent hyperbolic nanofluid with the influence of radiation and heat source sink parameters throughout a porous medium in a symmetric kind of channel that is, in addition, taken from the following references Safia and Afzal [5], Safia and Nedeem [6], Abbasi et.al [7], White [8], Shapiro et al.[9], Burns and Pareks [10], Mekheimer [11], Mekheimer and El Kot [12], Mekheimor and al –Arabi [13], Kothandapani et al.[14], Ali [15], Saffman [16], Nadeam and Akbar [17], Takabatake and Ayukawa [18], Khan and Shehzad [19], Latham [20], Robert [21], and Fung [22],the low-Reynolds assumption is the technique that is employed under a prolonged-wave length (small wave number).

2. The Mathematical Modeling of the Problem

Under the effect of radiation and heat source sink parameters, the peristaltic transport of hyperbolic tangent nanofluid in a microchannel with density ρ and variable viscosity μ is taken in consideration. Let $\bar{y} = \pm h$ be the right and left side wall borders,

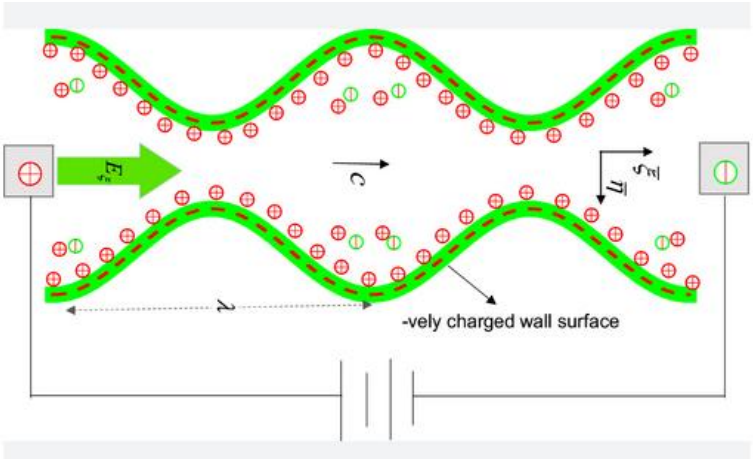

Figure A:

with a continuous tempo c throughout the length of the microchannel and the medium is deliciated that is attracted by a sinusoidal waveform, in fig. A, the right wall of declined channel preserved temperature T_0 and the volume of nanoparticle fraction C_0 while the left wall has temperature T_1 and the volume nanoparticle fraction C_1 , the geometry of the microchannel

is limited as the side of the channel wall has a width of 2d. It takes the form in the fixed reference frame ($\bar{X}, \bar{Y}$) as follows:

$\bar{H}_1(\bar{x},\bar{t}) = d_1 + \bar{a}_1 \cos^2\frac{\pi}{\lambda}(\bar{x} - c\bar{t})$.

$\bar{H}_2(\bar{x},\bar{t}) = - d_2 - \bar{a}_2 \cos^2[\frac{\pi}{\lambda}(\bar{x} - c\bar{t}) + \varphi]$. (1)

Where $\bar{a}$ the capacity of walls, λ wave-length, $\bar{t}$ dimensional time, and d represents wideness of the channel.

3. The Governing Equations of the Problem

The flow is governed by basic equations within electro hydrodynamics (EHD) of hyperbolic tangent nanofluid, that is unable to be compressed and given by the continuity equation:

$$\frac{\partial \bar{u}}{\partial \bar{x}} + \frac{\partial \bar{v}}{\partial \bar{y}} = 0 . \quad (2)$$

The momentum equations are:

$$\rho_f(\frac{\partial \bar{u}}{\partial \bar{t}} + \bar{u}\ \frac{\partial \bar{u}}{\partial \bar{x}} + \bar{v}\frac{\partial \bar{u}}{\partial \bar{y}}) = -\frac{\partial \bar{p}}{\partial \bar{x}} + \frac{\partial}{\partial \bar{x}}(\bar{s}_{\bar{x}\bar{x}}) + \frac{\partial}{\partial \bar{y}}(\bar{s}_{\bar{x}\bar{y}}) + \bar{s}_c E_x - \frac{\mu_\circ u}{k} \quad . \quad (3)$$

$$\rho_f(\frac{\partial \bar{v}}{\partial \bar{t}} + \bar{u}\ \frac{\partial \bar{v}}{\partial \bar{x}} + \bar{v}\frac{\partial \bar{v}}{\partial \bar{y}}) = -\frac{\partial \bar{p}}{\partial \bar{y}} + \frac{\partial}{\partial \bar{x}}(\bar{s}_{\bar{x}\bar{y}}) + \frac{\partial}{\partial \bar{y}}(\bar{s}_{\bar{y}\bar{y}}) - \frac{\mu_\circ v}{k} \quad . \quad (4)$$

The temperature equation is given by:

$$\rho c_p\ (\bar{u}\ \frac{\partial \bar{T}}{\partial \bar{x}} + \bar{v}\frac{\partial \bar{T}}{\partial \bar{y}}) = \kappa(\frac{\partial^2}{\partial \bar{x}^2} + \frac{\partial^2}{\partial \bar{y}^2})\bar{T} - \frac{\partial \bar{q}_r}{\partial \bar{y}} + \overline{Q_\circ} . \quad (5)$$

In which $\bar{s}_{\bar{x}\bar{x}}$, $\bar{s}_{\bar{x}\bar{y}}$ and $\bar{s}_{\bar{y}\bar{y}}$ are components of shear stress of hyperbolic tangent.
And the radiative heat of flux satisfy :

$$\bar{q}_r = -\frac{4\sigma'}{3k'}\frac{\partial \bar{T}^4}{\partial \bar{y}} \quad . \quad (6)$$

The difference in temperature within the flow, which is obviously seen, is small enough such like the expression $\bar{T}^4$ in Taylor free stream temperature series, $\overline{T_\circ}$ and terms of the higher order are neglected firstly in ($\bar{T} - \overline{T_\circ}$). Hence, replacing Eq. (6) we will have:

$$\bar{q}_r = -\frac{16\sigma' T_\circ^3}{3k'}\frac{\partial \bar{T}}{\partial \bar{y}} \quad . \quad (7)$$

4. Method of Solution:

For simplifying the governing equations of motion, temperature and condensation, the subsequent dimensionless alteration can be explained as :

$x = \frac{\bar{X}}{\lambda}$, $y = \frac{\bar{Y}}{d}$, $t = \frac{c\,\bar{t}}{\lambda}$, $u = \frac{\bar{U}}{c}$, $v = \frac{\bar{V}}{\delta\, c}$, $= \frac{d}{\lambda}$,

$h = \frac{\bar{H}}{d}$, $p = \frac{d^2\bar{P}}{c\lambda\bar{\mu}_\circ}$, $= \frac{\bar{T}-\bar{T}_\circ}{\overline{T_1}-\bar{T}_\circ}$, $\Phi = \frac{\bar{\Phi}}{\zeta}$, $a = \frac{\bar{a}}{d}$,

$\sigma = \frac{\bar{c}-\bar{c}_\circ}{\bar{c}_1-\bar{c}_\circ}$, $s_{xx} = \frac{d}{\bar{\mu}_\circ c}\bar{s}_{xx}$, $s_{xy} = \frac{d}{\bar{\mu}_\circ c}\bar{s}_{\bar{x}y}$,

$s_{yy} = \frac{d}{\bar{\mu}_\circ c}\bar{s}_{\bar{y}\bar{y}}$, $\dot{\gamma} = \frac{\bar{\dot{\gamma}}\,d}{c}$. (8)

Where x is axial assortment with no dimension, p pressure without dimension , u and v are axial that are non-dimensional and cross-cut velocity constituent, y is non-dimensional transverse coordinate, a is magnitude ratio, ζ is zeta prospective, θ is the dimensionless temperature, δ is wave number, and σ is the rescaled nanoparticle of volume fraction that is also dimensionless.

In this case, defining the connection between the stream function ψ and the velocity fields will be introduced as :

$u = \frac{\partial \psi}{\partial y}$, $v = -\frac{\partial \psi}{\partial x}$. (9)

When non-dimensional variables and parameters above have been used in (8), we will have the adjusted equations as:

$\frac{\partial u}{\partial x} + \frac{\partial v}{\partial y} = 0$. (10)

$$Re\delta\left(\frac{\partial^2}{\partial t\,\partial y} + \frac{\partial}{\partial y}\frac{\partial^2}{\partial x\,\partial y} - \frac{\partial}{\partial x}\frac{\partial^2}{\partial y^2}\right)\psi = -\frac{\partial p}{\partial x} + \delta\frac{\partial s_{xx}}{\partial x} + \frac{\partial s_{xy}}{\partial y} + Uhs\left(\delta^2\frac{\partial^2 \Phi}{\partial x^2} + \frac{\partial^2 \Phi}{\partial y^2}\right) + Gr\theta - k^2\frac{\partial \psi}{\partial y} \quad (11)$$

Where $k^2 = \frac{d^2}{k}$

$$- \quad Re\delta^3\left(\frac{\partial^2}{\partial t\partial x} + \frac{\partial}{\partial y}\frac{\partial^2}{\partial x^2} - \frac{\partial}{\partial x}\frac{\partial^2}{\partial x\partial y}\right)\psi = -\frac{\partial p}{\partial y} + \delta^2\frac{\partial s_{xy}}{\partial x} + \delta\frac{\partial s_{yy}}{\partial y} + k^2\delta^2\frac{\partial \psi}{\partial x} \quad . \quad (12)$$

$$- \quad Re\delta P_r\left(\frac{\partial \psi}{\partial y}\frac{\partial}{\partial x} - \frac{\partial \psi}{\partial x}\frac{\partial}{\partial y}\right)\theta = \delta^2\frac{\partial^2 \theta}{\partial y^2} + (1 + Rn)\frac{\partial^2 \theta}{\partial y^2} + \beta \quad . \quad (13)$$

Where $Re = \frac{\rho c d}{\bar{\mu}_\circ}$ is the Reynold number, $Uhs = -\frac{E_x \varepsilon \zeta}{\bar{\mu}_\circ c}$ is the Helmholtz-Smoluchowski velocity , $w_e = \frac{\Gamma c}{d}$ is the Weissenberg number, $\beta = \frac{\overline{Q}_\circ d^2}{(\bar{T}_1 - \bar{T}_\circ)\alpha_m}$ is the non-dimensional heat source / sink parameters, $p_r = \frac{\bar{\mu}_\circ c_f}{\alpha_m}$ is the Prandtl number. $N_t = \frac{\rho \acute{c}_p (\bar{T}_1 - \bar{T}_\circ) D_T}{T_m \alpha_m}$ is the parameter of thermophoresis, $Rn = -\frac{16\acute{\sigma}}{3\acute{k}\bar{\mu}_\circ c_f}$ is the parameter of radiation, $G_r = \frac{\rho g \beta_1 (\overline{T_1} - \bar{T}_\circ)}{c\bar{\mu}_\circ}$ is the local temperature Grashof number , and $Bh = \frac{h_b d}{k_b}$ the heat transfer Biot number at walls.

The assumptions have been employed of a long wavelength and low Reynolds number and disregarding the term of arrangement δ and highest, Equations. (11),(12),(13) will be:

$\frac{\partial p}{\partial x} = \frac{\partial}{\partial y}(1 + n(w_e\frac{\partial^2 \psi}{\partial y^2} - 1))\left(\frac{\partial^2 \psi}{\partial y^2}\right) + uhs\frac{\partial^2 \Phi}{\partial y^2} + Gr\theta - k^2\frac{\partial \psi}{\partial y}$. (14)

$\frac{\partial p}{\partial y} = 0$. (15)

$(1+Rn)\frac{\partial^2 \theta}{\partial y^2} + \beta = 0$. (16)

Derived equation (14) for y and equation (15) for x, terminating the term of pressure from eq.(14). It will be:

$\frac{\partial^2}{\partial y^2}(1 + n(w_e\frac{\partial^2 \psi}{\partial y^2} - 1))\left(\frac{\partial^2 \psi}{\partial y^2}\right) + Uhs\frac{\partial^3 \Phi}{\partial y^3} + Gr\frac{\partial \theta}{\partial y} - k^2\frac{\partial^2 \psi}{\partial y^2} = 0.$ (17)

Employing the linearization of Debye-Huckel, the equation of Poisson-Boltzmann decreased to:

$\nabla^2 \bar{\Phi} = k^2 \bar{\Phi}$. (18)

Taking advantage of the linearization of Debye-Huckel and non-dimensional equation of Poisson-Boltzmann can also resulted as:

$\frac{\partial^2 \Phi}{\partial y^2} = \kappa^2 \Phi$. (19)

5. Rate of Volumetric Flow and Boundary Conditions

In laboratory frame, the dimensional volume flow average is the instant volume flow average in the fixed frame that is given by:

$Q(\bar{X},\bar{t}) = \int_{-h(x,t)}^{h(x,t)} u(x,y,t)dy$. (20)

In wave frame, the equation above is

$F(x_w) = \int_{-h(x_w)}^{h(x_w)} u_w(x_w, y_w)dy_w$. (21)

In two frames, velocity and the coordinates (wave frames and laboratory) are related as:

$X = x_w - ct$, $y = y_w$, $u = u_w + c$, $v = v_w$. (22)

by Eqs. (20)- (22), we will have:

$Q = F + 2h(x)$. (23)

The time of averaged flow rate is recognized as $\Theta = \int_0^1 Q(x,t)dt$ furthermore, it can be derived as:

$\Theta = F + 2 + a$. (24)

The boundary conditions which are non-dimensional (boundary conditions that are connective) are used as:

$\psi = \frac{F}{2}$, $\frac{\partial \psi}{\partial y} = -1$, $\frac{\partial \theta}{\partial y} = Bh(1-\theta), \sigma = 1$,and $\Phi = 1$ at $y = h$

$\psi = -\frac{F}{2}$, $\frac{\partial \psi}{\partial y} = -1$, $\frac{\partial \theta}{\partial y} = Bh\theta, \sigma = 0$,and $\Phi = 0$ at $y = -h$. (25)

6. Solution of the Problem

6.1. Exact Solution

Solution of Equations (16) – (19) are submissive to boundary conditions introduced in Eqs. (25), the investigative solutions are obtained as:

$\Phi(y) = \frac{\sinh(h+y)k)}{\sinh(2hk)}$. (26)

$\theta(y) = c(cosh(\gamma_1 y) + \sinh(\gamma_1 y)) + D(\cosh(\gamma_2 y)) + \sinh(\gamma_2 y))$. (27)

$\sigma(y) = E + F_y - \frac{Nt}{Nb}(c(\cosh(\gamma_1 y) + \sinh(\gamma_1 y)) + D(\cosh(\gamma_2 y) + \sinh(\gamma_2 y))$. (28)

6.2. Disturbance Solution

Equation (16) and (19) are described to be differential and highly nonlinear equations. The solution has been acquired as a perturbation method for the stream function because it is not possible to get the investigative solution directly in term of small parameters *We* (Weissenberg number), by extending, p and F in the coming equation:

$\psi = \psi_\circ + w_e \psi_1 + O(\psi_2)$

$P = P0 + w_e p_1 + O(p_2)$

$F = F_\circ + w_e F_1 + O(F_2)$. (29)

In the above expressions, replacing in Equations. (17) and gathering the powers *We*, the system will be as follows:

$$\frac{\partial^2}{\partial y^2}\left(\frac{\partial^2\psi_\circ}{\partial y^2}+\mathrm{n}w_e\left(\frac{\partial^2\psi_\circ}{\partial y^2}\right)^2+\mathrm{n}w_e{}^2\frac{\partial^2\psi_\circ}{\partial y^2}\frac{\partial^2\psi_1}{\partial y^2}-\mathrm{n}\frac{\partial^2\psi_\circ}{\partial y^2}+w_e\frac{\partial^2\psi_1}{\partial y^2}+nw_e{}^2\frac{\partial^2\psi_\circ}{\partial y^2}\frac{\partial^2\psi_1}{\partial y^2}+nw_e{}^3\left(\frac{\partial^2\psi_1}{\partial y^2}\right)^2-nw_e\frac{\partial^2\psi_1}{\partial y^2}\right)+\mathrm{Uhs}\frac{\partial^3\Phi}{\partial y^3}+\mathrm{Gr}\frac{\partial\theta}{\partial y}-\mathrm{k}^2\frac{\partial u}{\partial y}=0. \quad (30)$$

6.2.1. For The System of Zero's- Order

$$\frac{\partial^4\psi_\circ}{\partial y^4}=\frac{\mathrm{uhs}}{n-1}\frac{\partial^3\Phi}{\partial y^3}+\frac{\mathrm{Gr}}{n-1}\frac{\partial\theta}{\partial y}-\frac{\mathrm{k}^2}{n-1}\frac{\partial^2\psi_\circ}{\partial y^2}. \quad (31)$$

$$\frac{\partial p_\circ}{\partial x}=(1-\mathrm{n})\frac{\partial^3\psi_\circ}{\partial y^3}+\mathrm{uhs}\frac{\partial^2\Phi}{\partial y^2}+\mathrm{Gr}\theta-\mathrm{k}^2\frac{\partial\psi_\circ}{\partial y} \quad . \quad (32)$$

$$\psi_\circ=\pm\frac{F_\circ}{2},\ \frac{\partial\psi_\circ}{\partial y}=-1\ ,\ \text{at y}=\pm\mathrm{h}\ . \quad (33)$$

6.2.2. For The System of First-Order

$$\frac{\partial^4\psi_1}{\partial y^4}=\frac{n}{n-1}\frac{\partial^2}{\partial y^2}\left(\frac{\partial^2\psi_\circ}{\partial y^2}\right)^2. \quad (34)$$

$$\frac{\partial p_1}{\partial x}=(1-\mathrm{n})\frac{\partial^3\psi_1}{\partial y^3}+\mathrm{n}\frac{\partial}{\partial y}\left(\frac{\partial^2\Phi}{\partial y^2}\right)^2-\mathrm{k}^2\frac{\partial\psi_1}{\partial y}. \quad (35)$$

$$\psi_1=\pm\frac{F_1}{2},\ \frac{\partial\psi_1}{\partial y}=0\ ,\ \text{at y}=\pm\mathrm{h}\ . \quad (36)$$

6.3. Temperature Equation Solution

In Eq.(16) the temperature solution satisfies the boundary conditions in Eq. (25) is found in the form of :

$$\theta[y]=c_1+yc_2-\frac{y^2\beta}{2(1+\mathrm{Rn})} \quad . \quad (37)$$

Where c_1, c_2 are fixed and can be quantified via employing the boundary conditions in Eq. (25) that is:

$$c_1=-\frac{-\mathrm{Bh}-2h\beta-\mathrm{Bh}h^2\beta-\mathrm{BhRn}}{2\mathrm{Bh}(1+\mathrm{Rn})},c_2=\frac{\mathrm{Bh}}{2(1+\mathrm{Bh}h)}. \quad (38)$$

6.4. For System Of Order (We^0) Solving

Eq. (31) solution is contented with the boundary conditions Eq. (33) can be inscribed as:

$$\psi_\circ(y)=c_5+yc_6+\frac{-6\mathrm{c3Cos}[\sqrt{\mathrm{t3}}y]+\frac{6\mathrm{t1t3t4}\kappa\mathrm{Cosh}[(h+y)\kappa]}{\mathrm{t3}+\kappa^2}-6\mathrm{c4Sin}[\sqrt{\mathrm{t3}}y]+\mathrm{t2}y^2(3\mathrm{c2}-\frac{y\beta}{1+\mathrm{Rn}})}{6\mathrm{t3}} \quad . \quad (39)$$

Eq. (32) solution is satisfying the boundary conditions , Eq. (33) can be inscribed as :

$$p_\circ=\mathrm{Uhs}\kappa^2\mathrm{Csch}[2\kappa(1-a(1-\mathrm{Cos}[x]^2))]\mathrm{Sinh}[\kappa(1+y-a(1-\mathrm{Cos}[x]^2))]+\mathrm{Gr}\left(\frac{\mathrm{Bh}y}{2\left(1+\mathrm{Bh}\left(1-a\left(1-\mathrm{Cos}[x]^2\right)\right)\right)}-\frac{y^2\beta}{2(1+\mathrm{Rn})}-\frac{-\mathrm{Bh}-2\beta\left(1-a\left(1-\mathrm{Cos}[x]^2\right)\right)-\mathrm{Bh}\beta\left(1-a\left(1-\mathrm{Cos}[x]^2\right)\right)^2-\mathrm{BhRn}}{2\mathrm{Bh}(1+\mathrm{Rn})}\right). \quad (40)$$

Where c_3 and c_4 are fixed can be obtained by employing boundary conditions in Eq. (33) and "MATHEMATICA" software :

$$c_3 = -\frac{\text{Csc}[h\sqrt{\text{t3}}](2\text{c2}ht2(\text{t3}+\kappa^2)+\text{t1t3t4}\kappa^2\text{Sinh}[2h\kappa])}{2\sqrt{\text{t3}}(\text{t3}+\kappa^2)}$$
$$c_4 = \frac{3F0t3^2+6ht3^2-2h^3t2t3\beta+3t1t3t4\kappa+3F0t3\kappa^2+\cdots}{6(t3+\kappa^2)(h\sqrt{t3}Cos[h\sqrt{t3}]-Sin[h\sqrt{t3}])(1+Rn)} \quad . \qquad (41)$$

6.5. For System Of Order (We^1) Solving

Eq. (34) solution is contented with the boundary conditions Eq.(36) can be formed as:

$$\psi_1 = c_7 + yc_8 + y^2c_9 + y^3c_{10} + \ldots \qquad (42)$$

Eq. (35) solution is satisfying the boundary conditions Eq.(36) can be formed as:

p_1= 1/(8 k^4) (-1+n)^2 n (-((2 Gr)/(-1+… (43)

Where c_7, c_8, c_9, c_{10} are fixed and can be quantified by employing boundary conditions in Eq. (36) and "MATHEMATICA" software.

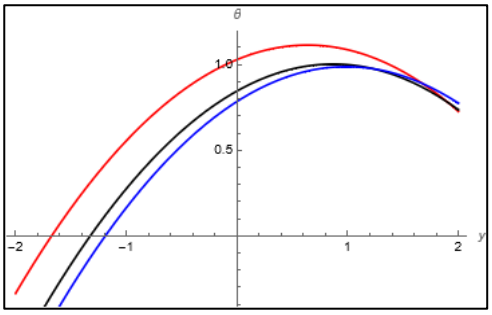

Figure 1: Temperature distribution for variation of β
$\text{Bh} = 1, \text{Rn} = 0.2, a = \text{Pi}/4$
(a) $\beta = 0.1$,(b) $\beta = 0.3$,(c) $\beta = 0.5$

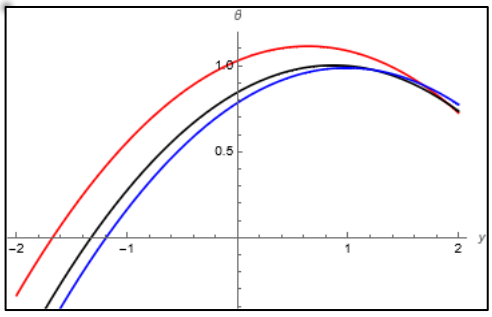

Figure 2 : Temperature distribution for variation of Bh
$\beta = 0.5, \text{Rn} = 0.2, a = \text{Pi}/4$
(a) $\text{Bh} = 1$,(b)$\text{Bh} = 2$,(c) $\text{Bh} = 3$

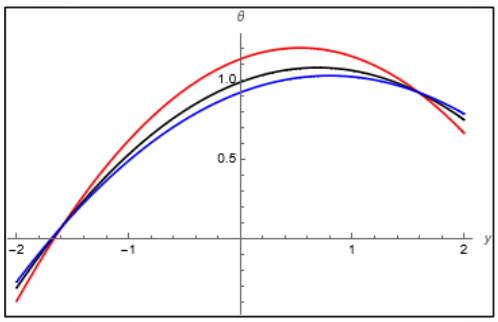

Figure 3: Temperature distribution for $a$variation of Rn
$\beta = 0.5, \text{Bh} = 1, \text{a} = \text{Pi}/4$,
(a)$\text{Rn} = 0$,(b) $\text{Rn} = 0.3$,(c) $\text{Rn} = 0.5$

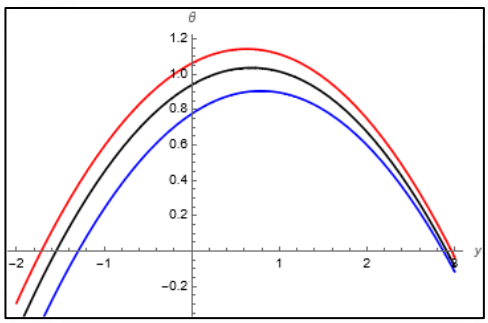

Figure. 4: Temperature division for variation of of a
$\beta = 0.5, \text{Bh} = 1, \text{Rn} = 0, a = \text{Pi}/4$,
(a)$a = \text{Pi}/6$,(b)$a = \text{Pi}/2$,(c)$a = \text{Pi}$

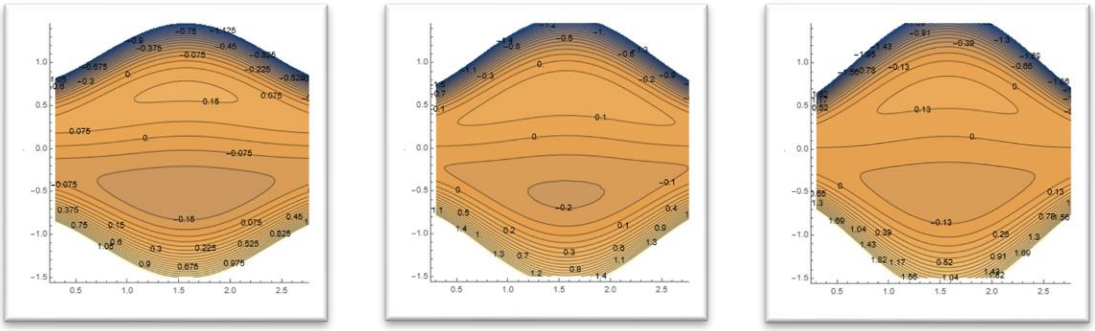

(Ⅰ) (Ⅱ) (Ⅲ)

Figure 5: stream line for $\mathrm{Bh} = 2$, $\mathrm{Rn} = 0.2, w_e = 0.05$, $\kappa = 1, \mathrm{Uhs} = 2$, $k = 2, \mathrm{Gr} = 2, n = 0.2$ (Ⅰ)$a = 0.6$ (Ⅱ) $a = 0.7$ (Ⅲ) $a = 0$.

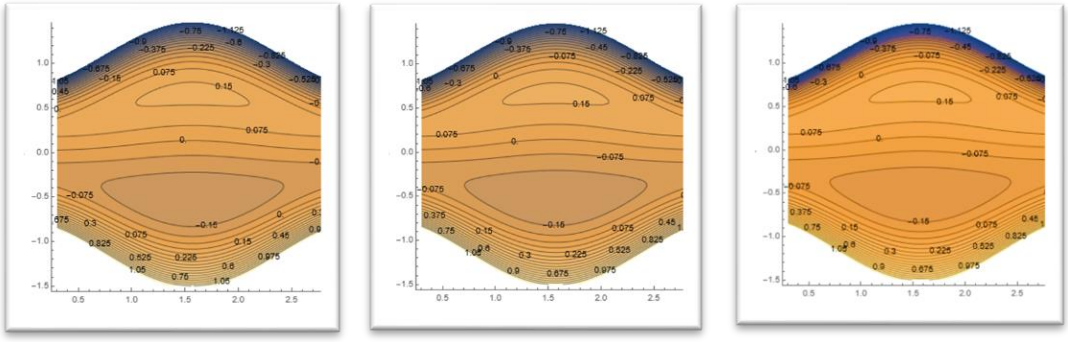

(Ⅰ) (Ⅱ) (Ⅲ)

Figure6: stream line for $\mathrm{Rn} = 0.2, a = 0.6$, $\mathrm{We} = 0.05$, $\kappa = 1$, $\mathrm{Uhs} = 2, k, Gr = 2, n = 0.2$

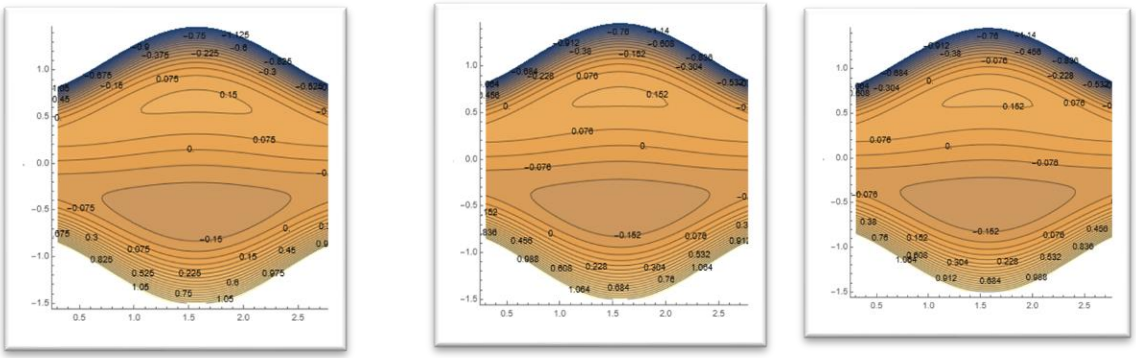

(Ⅰ) (Ⅱ) (Ⅲ)

Figure7: stream line for $Bh = 2, a = 0.6$, $\kappa = 1, \mathrm{Uhs} = 2, k = 2, \mathrm{Gr} = 2, n = 0.2, \beta = 1$ (Ⅰ)$\mathrm{Rn} = 0$(Ⅱ) $\mathrm{Rn} = 1$ (Ⅲ) $\mathrm{Rn} = 4$

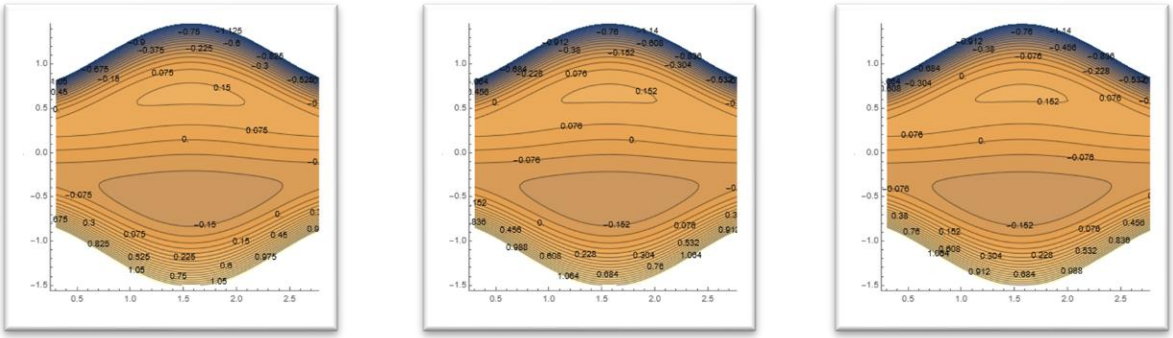

(Ⅰ) (Ⅱ) (Ⅲ)

Figure 8: stream line for $Bh = 2, a = 0.6$, $\mathrm{Rn} = 1$, $\kappa = 1$, $\mathrm{Uhs} = 2, k = 2, \mathrm{Gr} = 2, n = 0.2, \beta = 1$
(Ⅰ)$We = 0.05$ (Ⅱ) $We = 0.005$ (Ⅲ) $We = 0.0005$

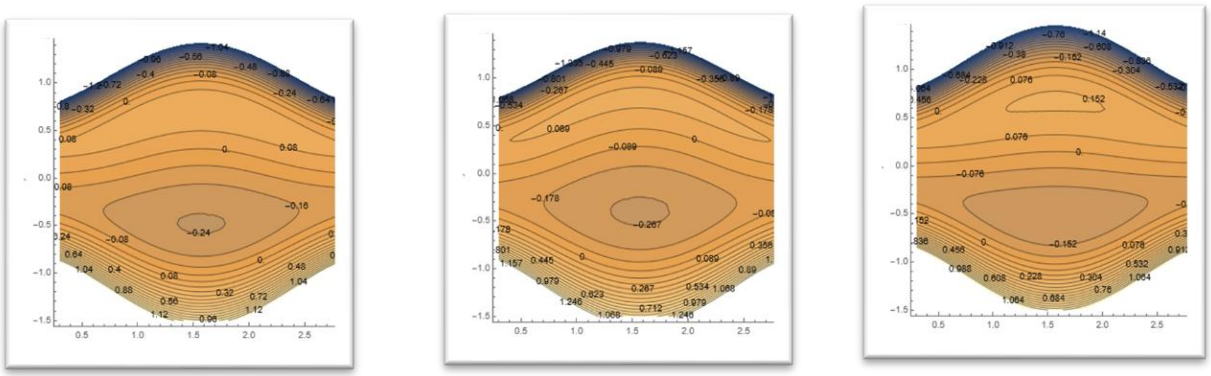

(Ⅰ) (Ⅱ) (Ⅲ)

Figure 9: stream line for $\mathrm{Rn} = 0.2, a = 0.6$, $\mathrm{We} = 0.05$, $\mathrm{Uhs} = 2, k = 2, \mathrm{Gr} = 2, n = 0.2, \beta = 1$
(Ⅱ) $\kappa = 2$(Ⅲ) $\kappa = 3$(Ⅰ)$\kappa = 1$

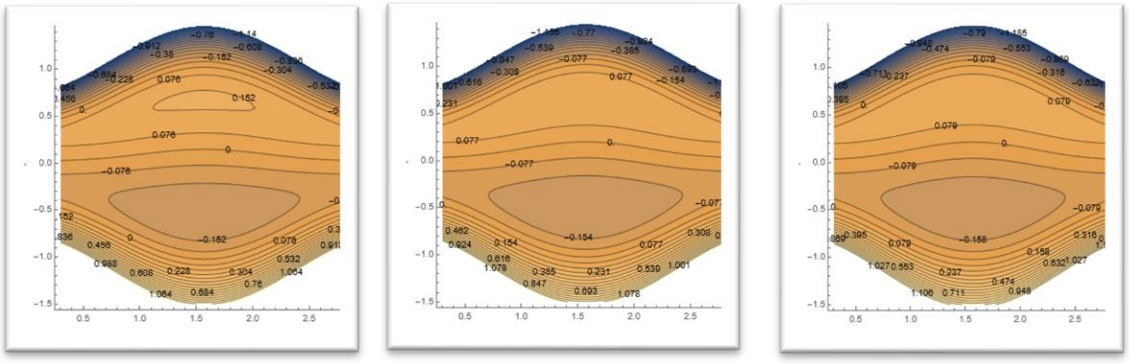

(I) (II) (III)

Figure 10: stream line for $\mathrm{Bh} = 2, \mathrm{Rn} = 1, a = 0.6$, $\mathrm{We} = 0.05$, $\kappa = 1, k = 2, \mathrm{Gr} = 2, n = 0.2, \beta = 1$ (Ⅰ)$\mathrm{Uhs} = 2$ (Ⅱ) $\mathrm{Uhs} = 3$ (Ⅲ) $\mathrm{Uhs} = 4$

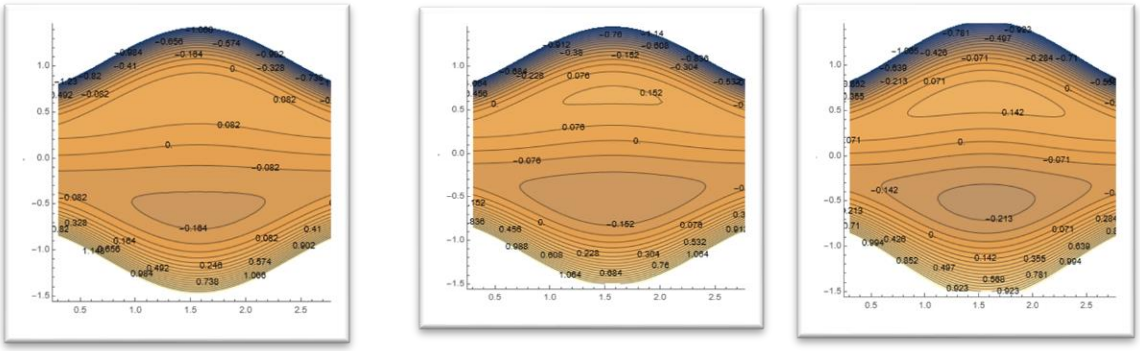

(Ⅰ) (Ⅱ) (Ⅲ)

Figure11: stream line for $\mathrm{Bh}=2, \mathrm{Rn}=1, a=0.6, \mathrm{We}=0.05, \kappa=1, \mathrm{Uhs}=2, \mathrm{Gr}=2, n=0.2, \beta=1$(Ⅰ)k = 1 (Ⅱ) k = 2 (Ⅲ) k = 3

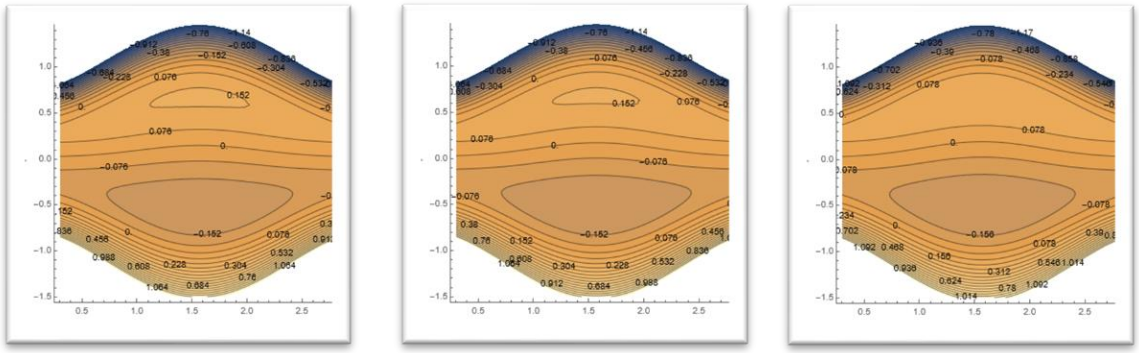

(Ⅰ) (Ⅱ) (Ⅲ)

Figure 12: stream line for $\mathrm{Bh}=2, \mathrm{Rn}=1, a=0.6, \mathrm{We}=0.05, \kappa=1, \mathrm{Uhs}=2, k=2, n=0.2, \beta=1$ (Ⅰ)Gr = 2 (Ⅱ) Gr = 3 (Ⅲ) Gr = 4

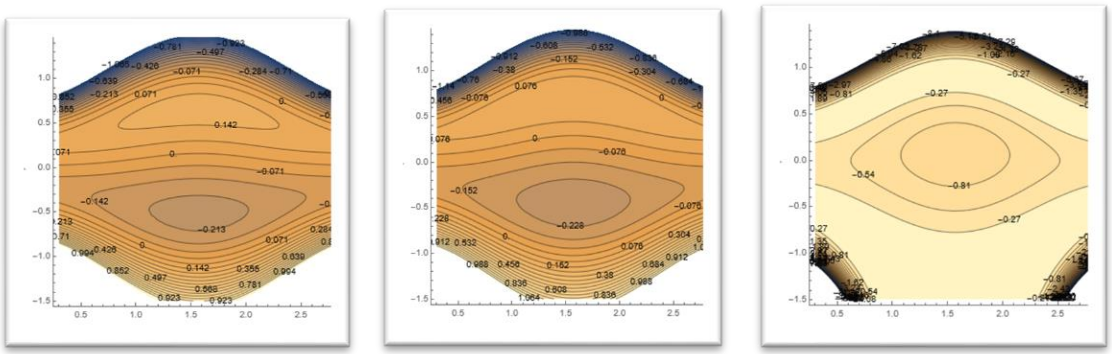

(Ⅰ) (Ⅱ) (Ⅲ)

Figure13: stream line for$\mathrm{Bh}=2, Rn=1, a=0.6, \mathrm{We}=0.05, \kappa=1, \mathrm{Uhs}=2, k=2, \mathrm{Gr}=2, \beta=1$(Ⅰ)n = 0.2 (Ⅱ) n = 0.5 (Ⅲ) n = 0.9

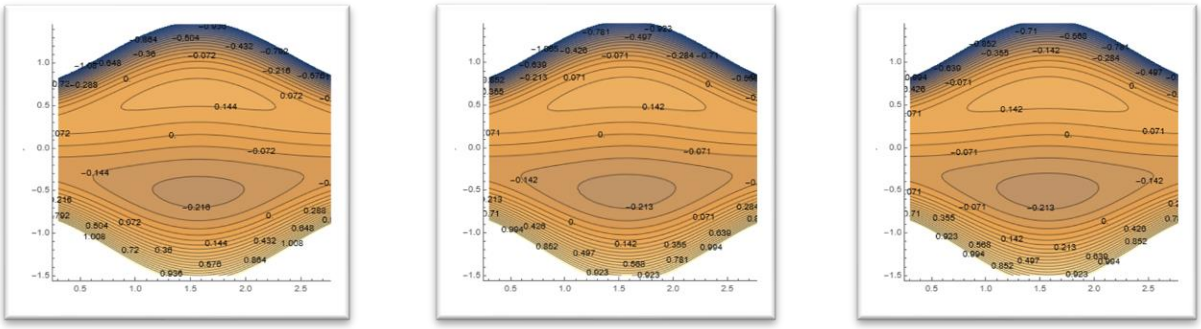

(Ⅰ) (Ⅱ) (Ⅲ)

Figure 14: stream line for $\mathrm{Bh}=2, Rn=1, a=0.6\,, \mathrm{We}=0.05\,, \kappa=1, \mathrm{Uhs}=2, k=1, \mathrm{Gr}=2$

(Ⅰ)$\beta=0.1$ (Ⅱ) $\beta=1$ (Ⅲ) $\beta=3$

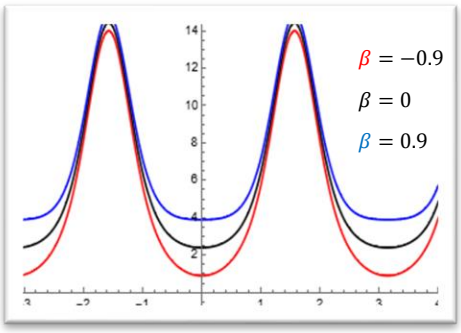

Figure 15: Pressure gradient for variation of β

$\mathrm{Bh}=1, \mathrm{Rn}=0.2, a=\mathrm{Pi}/8\,, \mathrm{We}=0.1, \kappa=1,$
$0.1, \kappa=1,$
$\mathrm{Uhs}=1, k=2, \mathrm{Gr}=2, n=0.2,$

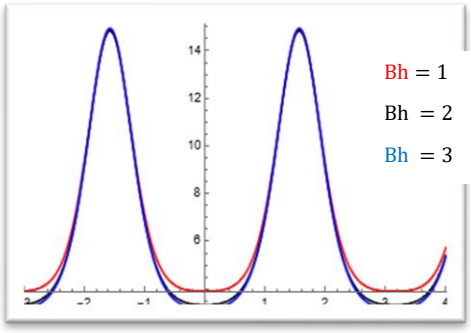

Figure 16: Variation of Bh of the pressure gradient

$\beta=0.9, \mathrm{Rn}=0.2, a=\mathrm{Pi}/8\,, \mathrm{We}=$

$\mathrm{Uhs}=1, k=2, \mathrm{Gr}=2$

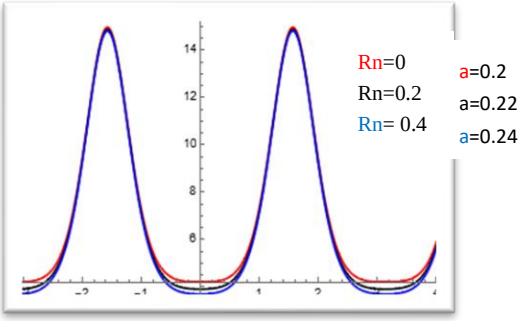

Figure 17: Pressure gradient for variation of Rn

$\beta=0.9\,, \mathrm{Bh}=1, a=\mathrm{Pi}/8\,, \mathrm{We}=0.1, \kappa=1,$
$\mathrm{Uhs}=1, k=2, \mathrm{Gr}=2, n=0.2$

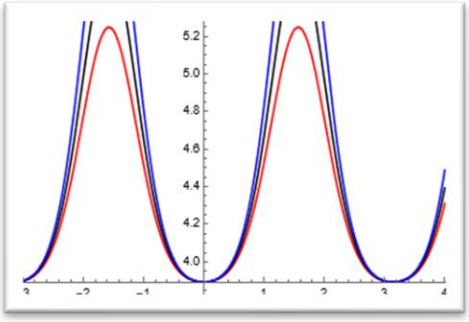

Figure 18: Pressure gradient for variation of a

$\beta=0.9, Bh=1, \mathrm{Rn}=0.2, \mathrm{We}=0.1$
$, \kappa=1,\ \mathrm{Uhs}=1, k=2, \mathrm{Gr}=2, n=0.2$

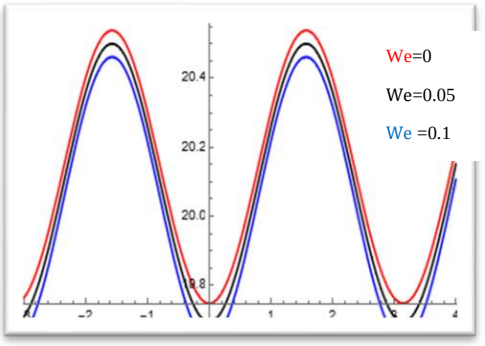

Figure19: Variation of pressure gradient for We $\beta = 0.1\,, Bh = 1, \mathrm{Rn} = 1, \mathrm{a} = 0.01, \kappa = 4.26,$ $\mathrm{Uhs} = 1, k = 2, \mathrm{Gr} = 2, n = 0.2$

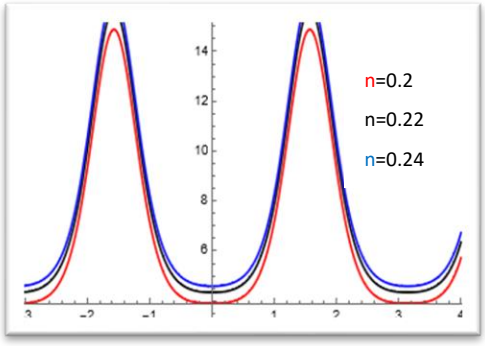

Figure20: Variation of pressure gradient for n $\beta = 0.9\,, Bh = 1, N_r = 0.2, \mathrm{a} = \mathrm{Pi}/8,$ $\kappa = 1,$ $\mathrm{Uhs} = 1, k = 2, \mathrm{Gr} = 2, n\ 0.2$

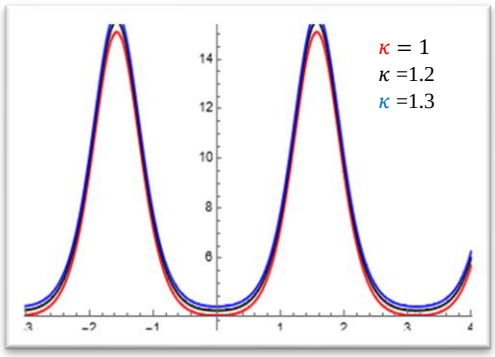

Figure 21: Variation of pressure gradient for κ $\beta = 0.9\,, Bh = 1, \mathrm{Rn} = 0.2, \mathrm{a} = \mathrm{Pi}/8\,, we = 0.1$ $\mathrm{Uhs} = 1, k = 2, \mathrm{Gr} = 2, n = 0.2$

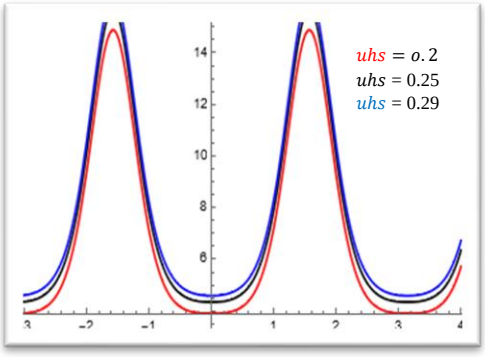

Figure 22: Variation of the pressure gradient $\beta = 0.9\,, Bh = 1, \mathrm{Rn} = 0.2, \mathrm{a} = \mathrm{Pi}/8\,, we = 0.1$ $\kappa = 2\,, k = 2, \mathrm{Gr} = 2, n = 0.2$

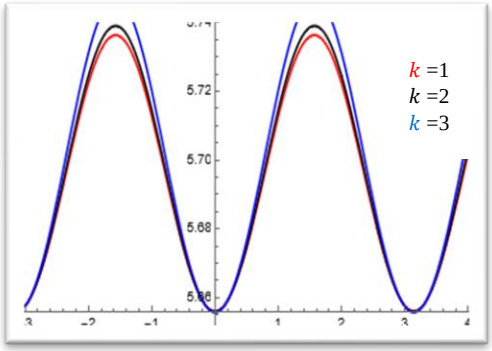

Figure 23 : Variation of pressure gradient for k $\beta = 0.1\,, Bh = 1, \mathrm{Rn} = 0.2, \mathrm{a} = 0.01, we = 0.01$ $\mathrm{Uhs} = 1, \kappa = 2, \mathrm{Gr} = 2, n = 0.2$

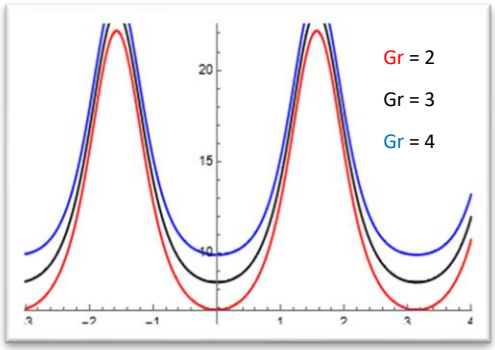

Figure(24): Variation of pressure gradient for Gr $\beta = 0.9\,, Bh = 1, \mathrm{Rn} = 0.2, \mathrm{a} = \mathrm{Pi}/8\,, we = 0.1$ $\kappa = 2\,, \mathrm{Uhs} = 1, k = 2, \mathrm{Gr} = 2, n = 0.2$

7. Results and Discussion

In this part, the numerical and computational results of the peristaltic transport problem of tangent hyperbolic nonliquids have been discussed in a channel that is tapered or asymmetric type, within the aid of non-slip utilizing states electroosmotic flow under the impact of heating and radiation of Joule through a porous medium.

Under the assumption of long wavelength and low Reynolds number approximations, analytical results have been presented by employing technique of small wave number δ value. Moreover, the use of series for stream functions, pressure gradient and flow rate mean F. The impacts are depicted graphically of various and important parameters

7.1. Pressure Gradient Distribution

The features of pumping are explicitly depending on deduced pressure gradient which is modulated via electroosmosis mechanism and generated via peristaltic pumping. The pressure gradient is immediately affected the flow rate that is volumetric, there is a relationship between the pressure gradient and the axial length of microchannel. Detour nature is curved inwards, the effect of these parameters has been numerically evaluated on Δp by employing "MATHEMATICA" program and the results are graphically depicted, figures (15) - (24) are found to examine the several vital parameter on pressure gradient. The fixed parameters values are gotten from the axial velocity profile. To examine the effects of the high temperature transfer Biot number (Bh = $\frac{h_b d}{k_b}$) on pressure gradient walls , In Figure (15) the impact of parameter of Joule heating β on pressure gradient Δp has been clearly noticed, and which is remarked in the pumping Δp, increasing in pressure gradient caused by an increase in β, in figure (16) the impact of transfer of heat Biot number Bh on Δp is seen. It has been observed that the decrease in the pressure gradient caused by an increase in Bh. In figure (17) the impact of thermal radiation principles Rn on Δp is observed. It has been examined that by increasing the thermal radiation**,** the pressure gradient decreases and the influence of (a) is observed clearly in figure (18). We observed that the increase of (a) causes an increase of pressure gradient. Furthermore, the pressure gradient decreases with the increase in the Weissenberg number and this can be observed in figure(19). In figures(20) and (21), it has been noted the pressure gradient increases with an increase of power law index (n) and electroosmosis parameter κ. Figure (22) shows the influence of Helmoholtz-Smoluchowski velocity (Uhs) on the pressure gradient. It can be clearly seen figure (22) that with the increase in Uhs, the pressure gradient increases, figure (23) is depicted to present the raising in the pressure gradient in case k is heightened. It is found that, from figure (24), with an increase of Grash number Gr, the value of pressure gradient increases.

7.2. Temperature Characteristics

To neatly observe the impact of several temperature parameters for constant values of x=0.4, temperature explanation obtained via Eq.(37) that is solved via precise solution and these parameters findings represented descriptively via employing "MATHEMATICA" program and depicted in figures(1)- (4), to compare the impact of different principles such as heat transfer Bh , β, Rn and a on nanoparticle volume fraction and thermal temperature in the medium of flow these figures are drawn.

Between transverse coordinate and thermal temperature/nanoparticle volume fraction, there is linear relationship that has been observed in the absence of Joule heating parameter.

Although, in the presence of heating parameter of Joule, it will be nonlinear relationship. To study the impact of (x=0.4) On temperature distribution, Figure (1) is drawn. It has been observed that the temperature magnitude reduced with the raising of β. Furthermore, it could be perceived that the raise of (Bh) leads to identical manner of impact on β, temperature as shown in figure (2). The influence of thermal radiation Rn on thermal temperature is shown in Figure (3). It has been perceived that the temperature magnitude reduces at the center and raises at the ends of channel. In figure (4), the temperature distribution for (a) is drawn, it is also clearly seen that within a raising in (a) the temperature reduces.

7.3. Streamline

In peristaltic transport, the trapping phenomenon is an essential topic, which can be explained as a formation of fluid circulating bolus throughout closed streamlines, along with the peristaltic waves which pushes ahead the trapped bolus. The phenomenon of trapping is shown in figures (5)-(14) for variant values of Bh , Rn , a , We , K , Uhs , Gr , n , β. In figure(5), the influence of (a) is seen, it is observed that the size and number of bolus are rising with raising of (a). The behavior of parameter Bh on bolus given in figure (6) which is clarified that with raising of Bh, the bolus is unchanged in shape.

In figure (7), the streams are shown for variant values of Rn. It is tested that with a raising of Rn size and a number of bolus increases. In figure (8) the streamlines are shown for several values of (We) . It is being noted that with a raise of (We) the size and number of bolus increases in the upper wall and reduces in the lower wall. figure(9) It has been noted that with a raise of κ ,in the upper wall of the channel the size of bolus is increased, and in the channel lower wall, the size of the bolus reduces. In figure (10), the different values of stream for Uhs are shown. It is observed that the size and number of bolus are rising with increase of Uhs. In figure (11) It has been noted that with a raise of K the bolus increase in size and number , In figure (12) It has been noted that with Gr raising , the sizes and number of bolus increase , In figure (13) It has been noted that with a raise of n the bolus increasing in size and number, In figure(14) the effects of β are plotted. the magnitude rises of β results small size and number of bolus in the upper wall and slight effect of β in the lower wall.

8. Conclusions

In this paper, it has been investigated the peristaltic transport of tangent hyperbolic nanofluid through a porous medium in a symmetric channel under the influence of radiation and heat source sink parameters. By choosing the peristaltic waves, the asymmetry channels are produced on the walls that a non-uniform to have variant phases and magnitude, low Reynolds number and long-wave length and estimations are applied. To get the expression for streamline, temperature and pressure gradient are employed.

For highest average in pressure over a wave length, numerical study has been conducted. The effects of Biot number of heat transfer (Bh) electroosmosis parameters (κ), power of law index (n), radiation parameter (Rn), Helmoholtz-Smoluchowski velocity (Uhs) , Weissenberg number (w_e), heat parameter of Joule (β) , porosity parameter (k), wave amplitudes (a) , and Prandtl number (Pr) on pressure gradient, temperature and streamlines are also discovered in detail. It found out that:

1. The pressure gradient over a wave length increase with an increase of , (a), n. κ , Uhs k and Gr .
2. The pressure gradient over a wave length decreases with an increases of Bh , Rn, *We*.
3. The temperature decreases with the increasing of β , Bh and (a) .

4. The temperature reduces with the raising of Rn at the center and raises at the ends of channel with the increases of Rn .
5. The size and number of trapping bolus increased with a raising of a, Rn, Uhs ,n , K and Gr .
6. The number and size of bolus in the upper wall of the channel raise, and in the lower wall of the channel, the size of bolus reduced with the raising of κ and We.
7. The number and size of bolus in the upper wall of the channel increase, and slight effect in the lower wall with raising of β.
8. bolus is unchanged in shape with raising of Bh.

References

[1] A.M. Abdulhadi and M. Sabah, "On Newtonian fluid flow Problem in Two Dimension Solving by Simple Algorithm", *Iraqi Journal of Science*,vol.51,no.4,pp.663,2011.

[2] A.M. Abdulhadi and M.A. Morad, "Unsteady Flow of Non-Newtonian Fluid in a Curved Pipe with Rectangular Cross-Section", *Iraqi Journal of Science*, vol.48,no.1,pp.182,2007.

[3] A.M. Abdulhadi and S.A.Fat'hy, "Two Dimensional Steady State Potential Flow Analysis by the BIE Method ", *Iraqi Journal of Science*,vol.36,no.4,pp.1239,1995.

[4] A.M. Abdulhadi and Q.K. Jawad, "Influence of MHD and Porous Media on Peristaltic Transport for Nanofluids in an Asymmetric Channel for Different Types of Walls," *Int. J. Nonlinear Anal. Appl.* In Press, pp. 1–14, 2022.

[5] A. Safia, F. Afzal and Q. Afzal, "Impact of Nanofluids and Magnetic Field on the Peristaltic Transport of a Couple Stress Fluid in an Asymmetric Channel with Different Wave Forms", *Islamabad, Pakistan, Sci*. vol.24 , no. 2, pp.1407–1414, 2019.

[6] A. Safia and S. Nadeem, "Influence of Induced Magnetic Field and Heat Transfer on the Peristaltic Motion of Jeffrey Fluid in an Asymmetric Channel with Closed Form Solutions", *Islamabad, Pakistan, J. , Magn. Magn. Mater.*,vol.328, 11-20,2013.

[7] F.M. Abbasi, M. Gul and S.A. Shehzad, "Effectiveness of Temperature-Dependent Properties of Au, Ag, Fe3O4, Cu Nanoparticles in Peristalsis of Nanofluids", Islamabad, Pakistan, Int. Commn. *Heat Mass Transf.*, vol.116, 104651,2020.

[8] F.M. White, "*Fluid Mechanics*", MC Graw-Hill Companies, Inc, New York, U.S.A.,1994.

[9] H.A. Shapiro, M. Y. Jaffrin and S. L. Weinberg, "Peristaltic Pumping with Long Wave Lengths at Low Reynolds Number", *J. Fluid Mech*. vol.37, 799-825,2006.

[10] J.C. Burns and J. Pareks, "Peristaltic Motion," *J. Fluid Mech.* , vol.29, pp.731-743,2006.

[11] Kh.S. Mekheimer,"Non Linear Peristaltic Transport of Magneto- Hydrodynamics Flow in an Inclined Planar Channel", *Arabian Journal for Science and Engineering*. vol.28,pp. 183-201,2003.

[12] Kh.S. Mekheimer and M.A. El Kot, "The Micro Polar Fluid Model for Blood Flow Through a Tapered Artery with Stenos," *Acta. Mech. Sin.* Vol.24, pp. 644-673,2008.

[13] Kh.S. Mekheimer and T.H, Al- Arabi," Non –Linear Peristaltic Transport of MHD Flow Through Porous Medium," *IJMMS*, vol.26,pp. 1663-1682,2003.

[14] M. Kothandapani and J. Prakash," Effects of Thermal Radiation Parameter and Magnetic Field on The Peristaltic Motion of Williamson Nano Fluid in a Tapered Asymmetric Channel," *Int. J. Heat Mass Trans.*, vol.81,pp. 234-245,2015.

[15] N. Ali, "*Perturbation Method*," New York, Wiley, 1999.

[16] P.G. Saffiman, "On the Boundary Condition at the Surface of Porous Medium, California Institute of Technology," *U.S.A., Stud, Appl. Math. So.*, pp. 93-101, 1971.

[17] S. Nadeem and N.Sh. Akbar, "Effects of Heat Transfer on the Peristaltic Transport of MHD Newtonian Fluid with Variable Viscosity: Application of a Domain Decomposition Method", *Islamabad, Pakistan, Communications in Non Linear Science and Numerical Simulation,* vol.14,pp. 3844-3855,2009.

[18] S. Takabatake and K. Ayukawa, "Numerical Study of Two-Dimensional Peristaltic Flows," *J. Fluid Mech.*,vol.122,pp.439-456,2006.

[19] S.U. Khan and S.A. Shehzad, "Electrical MHD Carreau Nanofluid Over a Porous Oscillatory Stretching Surface with Variable Thermal Conductivity: Applications of Thermal Extrusion

System", *COMSATS University Islamabad, Pakistan, Phys. A. Stat. Mech. Appl.*,vol.550,pp.124-132,2020.

[20] T. W. Latham, *Fluid Motion in Peristaltic Pump*, M. S. Thesis, Massachuestts Institute of Technology , Cambridge Massachusetts, U. S. A.,1966.

[21] W.F. Robert, T.Mc. Alan and J.P. Philip, *Introduction to Fluid Mechanics*, New York, John Wiley & Sons Inc, New York, U.S.A.,2004.

[22] Y.C. Fung, *Peristaltic Pumping a Bio Engineering Model: Proceeding of the Work Shop Ureteral Refilm Children*, National Academy of Science, Washington, D. C., U. S. A.,1971.